British Journal of Pharmacology (2007) 151, 888–899
 0007–1188/07 $30.00
www.brjpharmacol.org

RESEARCH PAPER

The nematode neuropeptide, AF2 (KHEYLRF-NH_2), increases voltage-activated calcium currents in *Ascaris suum* muscle

S Verma, AP Robertson and RJ Martin

Department of Biomedical Science, College of Veterinary Medicine, Iowa State University, Ames, IA, USA

Background and purpose: Resistance to all the classes of anti-nematodal drugs like the benzimidazoles, cholinergic agonists and avermectins, has now been recorded in parasites of animals and/or humans. The development of novel anthelmintics is an urgent and imperative need. Receptors of nematode neuropeptides have been suggested to be suitable target sites for novel anthelmintic drugs.
Experimental approach: To investigate the effect of AF2 on calcium-currents in *Ascaris suum* somatic muscle cells we employed the two-micropipette current–clamp and voltage–clamp techniques and a brief application of AF2.
Key results: Here we report the isolation of voltage-activated, transient, inward calcium currents. These currents are similar in characteristics to *Caenorhabditis elegans* UNC-2 type currents, non-L-type calcium currents. Following a 2-minute application of 1 μM AF2 , there was a significant long-lasting increase in the transient inward calcium current; AF2 increased the maximum current (from −84 nA to −158 nA) by shifting the threshold in the hyperpolarising direction (V_{50} changed from −7.2 to −12.8 mV) and increasing the maximum conductance change from 1.91 to 2.94 μS.
Conclusion and Implications: These studies demonstrate a mechanism by which AF2 increased the excitability of the neuromuscular system by modulating calcium currents in nematodes. A selective small molecule agonist of the AF2 receptor is predicted to increase the contraction and act synergistically with cholinergic anthelmintics and could counter resistance to these compounds.
British Journal of Pharmacology (2007) **151,** 888–899; doi:10.1038/sj.bjp.0707296; published online 21 May 2007

Keywords: AF2; *Ascaris suum*; calcium current

Abbreviations: 4-AP, 4-aminopyridine; cAMP, cyclic adenosine monophosphate; FLP, FMRFamide-like peptides; G_{max}, maximum conductance change; I_{max}, maximum current; K_{slope}, slope factor; PKA, protein kinase A; V_{50}, half maximum voltage

Introduction

Nematode parasites have a diverse biology and infect plants, insects, animals and humans. In most cases, they cause significant damage to their host. Chemical agents (anthelmintics) that have a selective toxic effect on the parasites have been developed to control and treat these infections. In most cases, these drugs were produced for domestic animal use, before they were developed for human use. This can be explained by the fact that the market for antiparasitic drugs in animals ($4 billion US world sales) is bigger than the market for human treatment ($0.5 billion US world sales). Regrettably, resistance to all the classes of antinematodal drugs like the benzimidazoles, cholinergic agonists and avermectins, has now been recorded in parasites of animals and/or humans (Dent *et al*., 2000; Geerts and Gryseels, 2001; Geary *et al*., 2004; Wolstenholme *et al*., 2004; Martin *et al*., 2005). The development of novel anthelmintics is an urgent and imperative need.

Beginning with AF1 and AF2, a series of more than 20 novel neuropeptides has been isolated from the parasitic nematode *Ascaris suum* (Stretton *et al*., 1991). Receptors of nematode neuropeptides have been suggested to be suitable target sites for novel anthelmintic drugs (Greenwood *et al*., 2005; Mousley *et al*., 2005). Neuropeptides, known as FMRFamide-like peptides (FLPs), possess a C-terminal motif usually comprising of an aromatic residue, a hydrophobic residue and an Arg-Phe-amide (Maule *et al*., 2002). These neuropeptides modulate neuromuscular function. The neuromuscular system is a recognised target for the nicotinic and avermectin anthelmintics. Evidence has also been gathered (Mousley *et al*., 2005) that shows that FLPs have

Correspondence: Dr RJ Martin, Department of Biomedical Sciences, College of Veterinary Medicine, Iowa State University, Ames, IA 50011, USA.
E-mail: rjmartin@iastate.edu
Received 8 January 2007; revised 16 March 2007; accepted 26 March 2007; published online 21 May 2007

activities in an extensive range of nematode parasites and even activities in arthropods. Although initially, it was considered that FLP receptors were not present in vertebrate hosts (Geary *et al*., 1999), it has now been recognised that a number of FLPs have physiological effects in vertebrates, including modulation of food intake (Dockray, 2004), antinociception (Pittaway *et al*., 1987) and increased blood pressure (Thiemermann *et al*., 1991). Despite the possibility that there are FLP receptors in vertebrates, there is still optimism that selective small ligands may be found and developed for antiparasitic use (Mousley *et al*., 2005; Greenwood *et al*., 2005).

AF2 is the FLP that has been recovered in greatest quantities from *A. suum* (Cowden and Stretton, 1993), *Caenorhabditis elegans* (Marks *et al*., 1995), *Haemonchus contortus* (Marks *et al*., 1999), and *Panagrellus redivivus* (Maule *et al*., 1994). AF2 has pronounced effects on muscle contraction of nematodes. At concentrations $>1\,\mu$M, AF2 produces excitatory responses in nematodes (Cowden and Stretton, 1993). The abundance of AF2 in very diverse nematodes and the effects on the nematode neuromuscular system suggest that AF2 receptors should be suitable targets for novel broad-spectrum anthelmintics. Consequently, we have continued the exploration of the effects of AF2 and found that brief pulse application potentiates the contractile effects of acetylcholine on *A. suum* muscle strips (Trailovic *et al*., 2005). We have also observed that it increased spike frequency in electrophysiological experiments suggesting effects on voltage-activated currents.

We have now tested this hypothesis using voltage–clamp to examine these currents in muscle cells of the parasitic nematode *A. suum*. Here, we report effects of AF2 on voltage-activated currents in *A. suum* muscle. We found that, following application of AF2, there was a long-lasting increase in the transient inward calcium current. These studies are important, because they demonstrate a mechanism by which AF2 increases the excitability of the neuromuscular system of nematodes. A selective small molecule agonist of the AF2 receptor is predicted to increase contraction and act synergistically with cholinergic anthelmintics and could counter development of resistance to these compounds.

Methods

Collection of worms

Adult *A. suum* were obtained weekly from the IBP pork packing plant at Storm Lake City, Iowa. Worms were maintained in Locke's solution (NaCl (155 mM), KCl (5 mM), $CaCl_2$ (2 mM), $NaHCO_3$ (1.5 mM) and glucose (5 mM)) at a temperature of 32°C. The Locke's solution was changed daily and the worms were used within 4 days of collection.

Muscle preparation

Muscle tissue flaps (1 cm) were prepared by dissecting the anterior part of the worm, 2–3 cm caudal to the head. A body muscle flap preparation was then pinned onto a Sylgard-lined 3 ml Petri-dish. The intestine was removed to expose the muscle cells. The preparation was continuously perfused, unless otherwise stated, with a calcium-Ringer containing 4-aminopyridine to reduce potassium currents with the following composition (mM): NaCl 23, Na acetate 110, KCl 24, $CaCl_2$ 6, $MgCl_2$ 5, glucose 11, HEPES 5 and 4-aminopyridine 5; NaOH was used to adjust the pH to 7.6. The preparation was maintained in the experimental chamber at 34°C using a Warner heating collar (DH 35) and heating the incoming perfusate with a Warner instruments (TC 324B) in line heating system (Hamden, CT, USA). The perfusate was applied at 4–6 ml min^{-1} through a 19-gauge needle placed directly over the muscle bag recorded from. Calcium substitution experiments were performed using a magnesium-Ringer (composition in mM: NaCl 23, Na acetate 110, KCl 24, $MgCl_2$ 11, glucose 11, HEPES 5, 4-aminopyridine (4-AP) 5 mM, and EGTA 0.5; NaOH was used to adjust the pH to 7.6). The sodium and calcium substitution experiments were conducted using *N*-methyl D-glucamine (NMDG)-Ringer (composition in mM: NMDG Cl 23, NMDG-acetate 110, KCl 24, $MgCl_2$ 11, glucose 11, HEPES 5 and 4-aminopyridine 5; CsOH was used to adjust the pH to 7.6). AF2 ($1\,\mu$M), verapamil ($100\,\mu$M), nickel ($30\,\mu$M) and cobalt (10 mM) were applied in calcium-Ringer as described in results.

Electrophysiology

Two-micropipette voltage–clamp and current–clamp techniques were employed to examine the electrophysiological effects in the *Ascaris* muscle bag region (Figure 1). Borosilicate capillary glass (Harvard Apparatus, Holliston, MA, USA) micropipettes were pulled on a Flaming Brown Micropipette puller (Sutter Instrument Co, Novato, CA, USA) and filled with 3 M potassium acetate or mixture of 1.5 M potassium acetate and 1.5 M cesium acetate. The cesium acetate was included in pipette solution to block outward potassium currents. Current–clamp micropipettes and the voltage-sensing micropipettes for voltage–clamp had a resistance of 20–30 MΩ; the current-injecting micropipette for voltage–clamp had a resistance of around 4 MΩ. The recordings were obtained by impaling the bag region of the *Ascaris* muscle with both of the micropipettes. All experiments were performed using an Axoclamp 2B amplifier, a 1320A Digidata interface and pClamp 8.2 software (Axon Instruments, Sunnyvale, CA, USA). All data were displayed and analysed on a Pentium IV-based desktop computer.

Current–clamp experiments were performed by injecting a hyperpolarising pulse of 40 nA for 500 ms at 0.28 Hz frequency through the current-injecting micropipette and the other micropipette recorded the change in membrane potential. Cells with stable resting membrane potentials over a period of 30 min and input conductance of less than $2.5\,\mu$S were used for analysis.

For voltage–clamp, the amplifier gain was set to more than 100 for all recordings. We also took extra care to keep the resistance of the current-injecting micropipette low (4 MΩ) and keeping the amplifier gain high. The phase lag was set to 1.5 ms in all the experiments to limit oscillation. In addition, muscles closer to the nerve cord were impaled for experi-

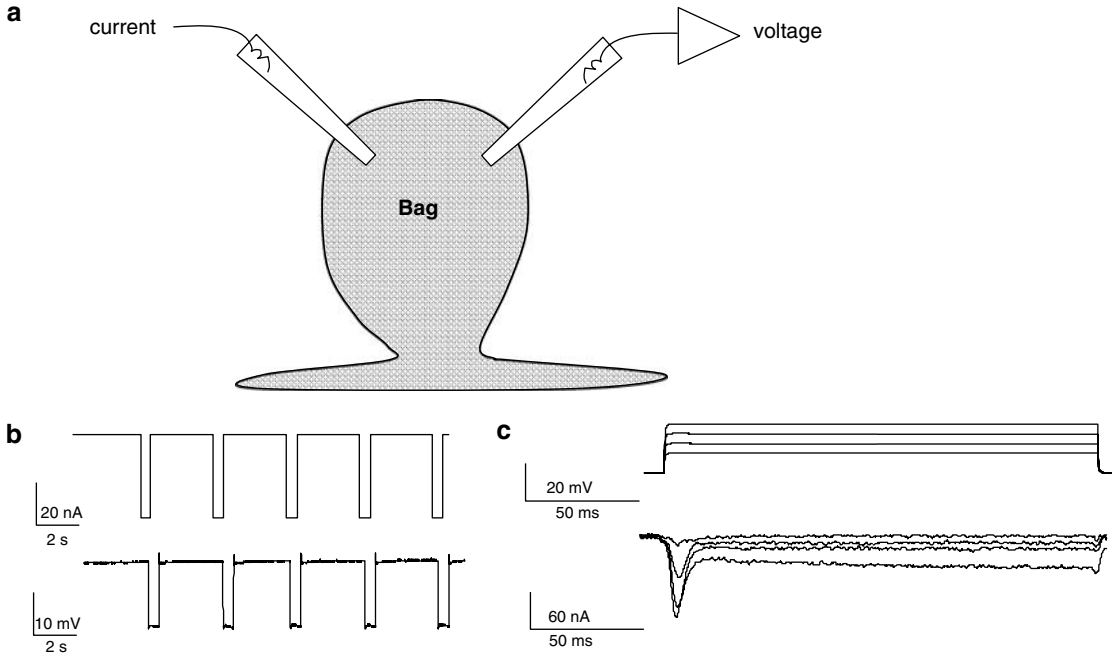

Figure 1 Electrophysiological techniques. (**a**) Diagram of the location of two micropipettes for making current–clamp and voltage–clamp recordings from bag region of *Ascaris suum* somatic muscle. (**b**) Current–clamp recording showing membrane potential change (lower trace) in response to 0.5 s, 40 nA, current pulses (upper trace). Input conductance 3.7 μS. (**c**) Voltage–clamp recording showing current responses (leak subtracted lower trace) in response to depolarising potentials from a holding potential of -35 mV. Note the presence of the voltage-activated transient inward current and a sustained current. Sustained currents were not prominent in all cells.

mental study, as they were rounder muscle cells with short arms to keep the space–clamp effective. Muscle cells close to the nerve cord were also found to possess bigger calcium currents.

For activation of calcium currents, muscle cells were held at -35 mV during the voltage–clamp experiments and stepped through a series of voltage-steps that increased by 5 mV and lasted 130 ms. The protocol had step potentials of -25, -20, -15, -10, -5, 0, $+5$, $+10$, $+15$ and $+20$ mV. In separate experiments, we studied the steady-state inactivation kinetics of the calcium current. We used conditioning pre-pulses of 130 ms that were applied before the step potential 0 mV. To investigate outward currents, step potentials of -25, -15, -5, $+5$, $+15$ and $+25$ mV were used lasting 200 ms. The holding potential again was -35 mV. The currents displayed were leak-subtracted using five 1 mV depolarising steps that were scaled by the pClamp 8.2 software.

Drugs were applied initially under current–clamp before effects on voltage-activated currents were tested under voltage–clamp. Cells with uniform membrane potentials more negative than -25 mV over a period of 40 min and resting conductance of less than 3 μS over the course of experiment were selected for the voltage–clamp studies.

Data analysis

Currents were plotted against the function of step potential to determine current–voltage relationships. For inactivation curves, peak-current values were plotted against the pre-pulse potentials. Results are given as means $\pm$ s.e.m., unless otherwise stated. The statistical analysis used Graph Pad Prism software (version 4.0, San Diego, CA, USA). The paired *t*-test was used to test significant difference in peak-current response in control and test recordings; significance levels were set at $P<0.05$. Two-way ANOVA with the *F*-test was used to compare the rates of rise of the small and large spikes.

Drugs

An AF2 (Sigma-Genosys, Woodland, TX, USA) 3 mM stock solution was prepared every week and kept in 1.5 ml microcentrifuge tubes at -12°C and used only once for one experiment after thawing. The AF2 solution was thawed just before use to make up the 1 μM AF2 for the experiments. A 100 μM verapamil solution was prepared fresh for each experiment. Cobalt chloride stock (100 mM) was prepared every week. Fresh 30 μM nickel and 1 μM acetylcholine solution was prepared for every experiment. All drugs were obtained from Sigma-Aldrich, St Louis, MO, USA. All the stock solutions were made using double-distilled water.

Results

AF2 increases the frequency and rates of rise of small spikes and large spikes under current–clamp

In a sample of 18 muscle cells from different preparations, 12 cells, defined as 'active' showed the presence of depolarising small spikes and large spikes before or following AF2 treatment (Weisblat *et al.*, 1976). In the remaining six 'quiet' preparations, the membrane potential showed no sponta-

neous depolarisations during the period of the experiment. The effect of a 2 min application of 1 μM AF2 on the resting membrane potential and input conductance on the 12 active muscle cells was a small but statistically significant ($P=0.03$, *t-test*) depolarisation without a noticeable effect on input conductance. In these 12 experiments, before the application of AF2, the resting membrane potential was 31.6 ± 2.1 mV and the input conductance was 2.66 ± 0.14 μS; after application of AF2, the membrane potential was 29.5 ± 1.6 mV with an input conductance of 2.68 ± 0.12 μS. In six quiet preparations, AF2 had no detectable effect on membrane potential or input conductance.

AF2 produced an increase in the frequency of small spikes and large spikes in the 12 active preparations. In five of these preparations, spiking was present before AF2 treatment, Figure 2a and b. In the remaining seven preparations, spiking was only present after AF2 treatment. Figure 2 shows an experiment where the large spike frequency increased from 0.03 spikes s^{-1} before AF2 to 0.1 spikes s^{-1} after AF2; and the small spikes frequency increased from 0.08 to 0.15 spikes s^{-1} after AF2.

AF2 also produced an increase in the rate of rise of the small spikes and the large spikes. In Figure 2a and b, the small spike rate of rise was 0.05 to 0.06 V s^{-1} before AF2 and 0.08 to 0.09 V s^{-1} after AF2; the rate of rise of the large spikes was between 1.2 to 1.4 V s^{-1} before AF2 and after AF2, the rate of rise increased to 1.3 to 1.7 V s^{-1}. Statistical analysis of the rates of rise of small spikes and large spikes for the five active preparations, where spiking was present before, as well as after AF2 treatment, showed that there was a significant ($P<0.001$, $F=210$, *df 1, 36*) increase in the rate of rise of the small spikes from 0.053 ± 0.002 to 0.084 ± 0.002 V s^{-1}, and that there was a significant ($P<0.001$, $F=96$, *df 1, 36*) increase in the rate of rise of the large spikes from 1.35 ± 0.02 to 1.50 ± 0.03 Vs^{-1}. The increased rates of rise of both of the spikes suggested that AF2 increased voltage-activated inward currents. Consequently, we explored the effects of AF2 under voltage–clamp as described in the experiments below.

Effects of AF2 on voltage-activated currents

Following our observations on the effect of AF2 on small and large spikes, we investigated effects on voltage-activated currents by switching the recording system to the voltage–clamp mode. Figure 3a shows initial records of total voltage-activated currents. These currents possessed: (1) an initial transient inward current, more visible at a step potential of 0 mV; and (2) a larger sustained outward potassium current, more visible at a step potential of + 25 mV (Thorn and Martin, 1987).

Effects of AF2 on voltage-activated currents were not observed during application of AF2, but increased in a time-dependent manner after AF2 application. Figure 3 shows effects of a 2-min application of 1 μM AF2 after a delay of 4 min. AF2 produced a small reduction in the peak outward current, but a larger increase in the transient inward current (Figure 3a and b). The outward peak current at the + 25 mV

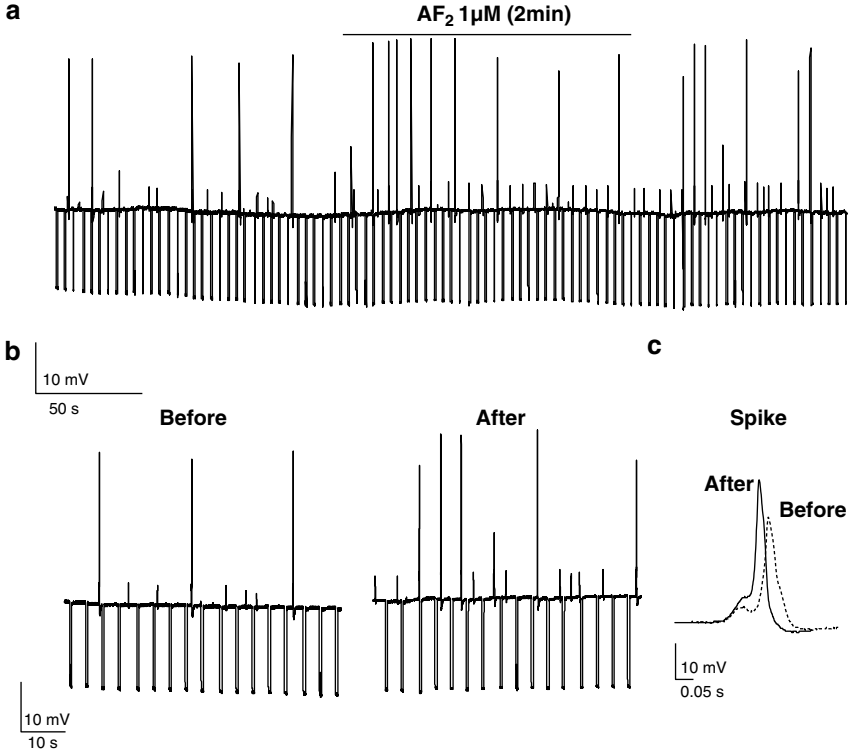

Figure 2 Effect of AF2 under current–clamp. Brief application of AF2 increases frequency of small and large spikes. (**a**) Membrane potential record of somatic muscle in current–clamp before, during and after application of 1 μM AF2. (**b**) The large spike frequency increased from 0.03 spikes s^{-1} before AF2 to 0.1 spikes s^{-1} after AF2; the small spike frequency increased from 0.08 to 0.15 spikes s^{-1}. (**c**) Represents the increase in the amplitude and rate of rise of large-spike before and after application of 1 μM AF2.

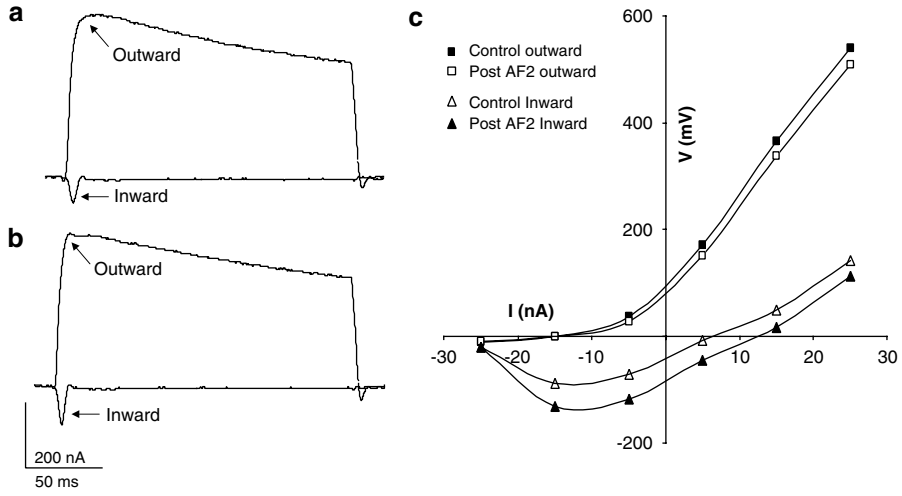

Figure 3 Effect of 2-min application of 1 μM AF2 on voltage-activated currents. (**a**) Control voltage-activated currents; peak outward currents and peak inward currents (under K^+ current block). (**b**) Voltage-activated currents following AF2 treatment. Note the slight decrease in the peak outward current and the increase in the peak inward current. (**c**) Current–voltage plot of the peak outward currents and the peak inward currents before, and following the 2-min application of 1 μM AF2. Note that proportionately, the biggest effect was on the peak inward current.

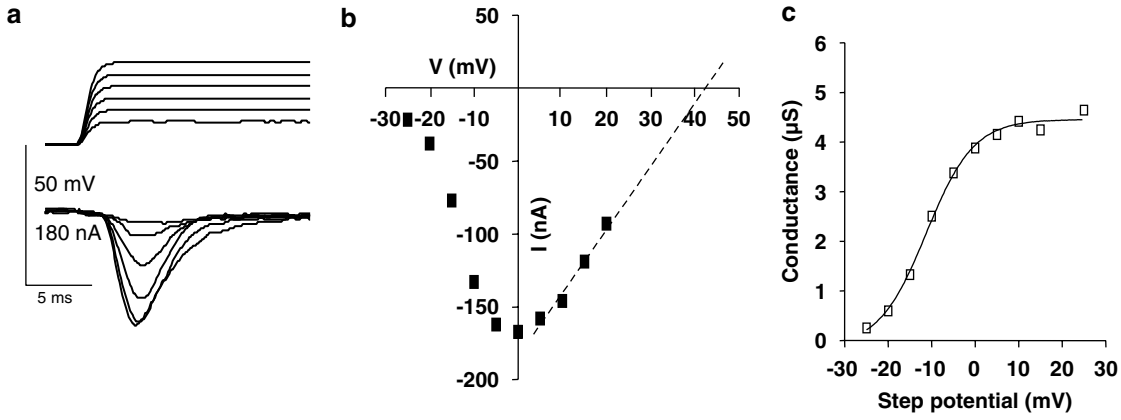

Figure 4 Activation curve of transient inward currents. (**a**) Voltage–clamp records following depolarising steps. Cell was held at −35 mV, and depolarising steps from −35 to +20 mV were made. Top trace: voltage steps. Lower trace: leak subtracted current records. (**b**) Peak inward current *vs* step-potential plot from same cell as (**a**) Step-potentials: −25, −20, −15, −10, −5, 0, +5, +10, +15 and +20 mV. The current-voltage relationship was extrapolated to predict reversal potential, +42 mV. (**c**) Activation curve for experiment shown in (**a**) and (**b**), fitted to Boltzmann equation.

voltage-step was 315±81 nA and this decreased significantly to 304±77.2 nA ($P=0.04$ paired *t-test*, $n=5$). The small effect of AF2 on the current–voltage plot of the outward peak currents is shown in Figure 3c. When we examined the peak transient inward current at 0 mV, we found that it increased significantly from −224±24 to −260±26 nA ($P=0.016$, paired *t-test*, $n=5$). Thus, we observed the effects of AF2 on the two currents and that the effect on the transient inward current was proportionately bigger than on the outward current.

Our next step was to separate the transient inward current from the outward current. We did this by using cesium in the recording micropipettes and adding 5 mM 4-AP to the bathing solution to block potassium currents. Also, we changed the voltage protocol to examine the activation of the inward current, in more detail; we increased the number of depolarising voltage-steps to every 5 mV and shortened the length of the voltage-steps from 200 to 120 ms.

Activation of the transient inward currents

The muscle cells were held at −35 mV. Figure 4a is a representative recording of the voltage-activated inward currents, where the outward potassium currents were blocked by 5 mM 4-AP applied in the bath and cesium in the recording micropipettes. The currents were characterised by a large transient inward current and a small sustained inward current that was <10% of the peak.

Figure 4b shows that the peak inward current was induced by a step potential to 0 mV. A similar observation was made in 16 preparations. The peak current-voltage relationship was extrapolated to predict the reversal potential (E_{rev}) for

each experiment. In the experiment shown in Figure 4b, we used linear regression and extrapolation to estimate the reversal potential (+42 mV) and then the calculated conductance changes from the peak inward currents and driving forces (E_{rev}–V) to obtain the activation curve, Figure 4c. The activation curve was then fitted by the Boltzmann equation:

$$G = G_{max}/\{1 + \exp[(V_{50} - V)/K_{slope}]\}$$

Where G is the conductance change, G_{max} is the maximum conductance change, V_{50} is the half-maximum step-voltage, V is the step-voltage and K_{slope} is the slope factor. For the experiment in Figure 4C, V_{50} was -11.3 ± 0.8 mV, G_{max} was 4.5 ± 0.1 μS and the slope factor was 5.5 ± 0.7 mV. In eight similar experiments, V_{50} ranged between –13.3 and -7 mV, G_{max} ranged between 1.7 and 4.5 μS, and the slope factor ranged between 4.5 and 7.5 mV. We discuss the characteristics of different calcium currents later.

Effect of AF2 on transient inward currents

Figure 5a shows a representative experiment of effects following a 2-min application of 1 μM AF2 on the peak transient inward current. We followed the same analytical approach as before to prepare the activation curves and to test the effect of AF2 on the transient inward currents. Figure 5a–d shows that AF2 increased the current by shifting the activation curve to the left and increasing the maximum conductance change. The peak current at the 0 mV step increased from -84 nA in the control to -158 nA after AF2 application (Figure 5a and b). The control activation curve had a V_{50} of -7.2 ± 0.4 mV and a G_{max} of 1.91 ± 0.02 μS. After AF2, V_{50} was -12.8 ± 0.4 mV and the G_{max} was 2.94 ± 0.03 μS (Figure 5c). Thus, there was a hyperpolarising shift of 5.4 mV in V_{50} and a 52% increase in G_{max} in this experiment. The slope factor for the curve changed from the control 7.0 ± 0.4 to 4.4 ± 0.3 mV after application of AF2.

It was clear from the experiment described in Figure 5a–c and from similar observations in 10 other experiments that AF2 increased the transient inward current. We were interested in determining the time-dependent nature and duration of this effect. To do this, we measured the percentage increase in the inward peak current at the 0 mV step-potential and followed this every 4 min. We found that the potentiation took at least 8 min to reach a maximum and

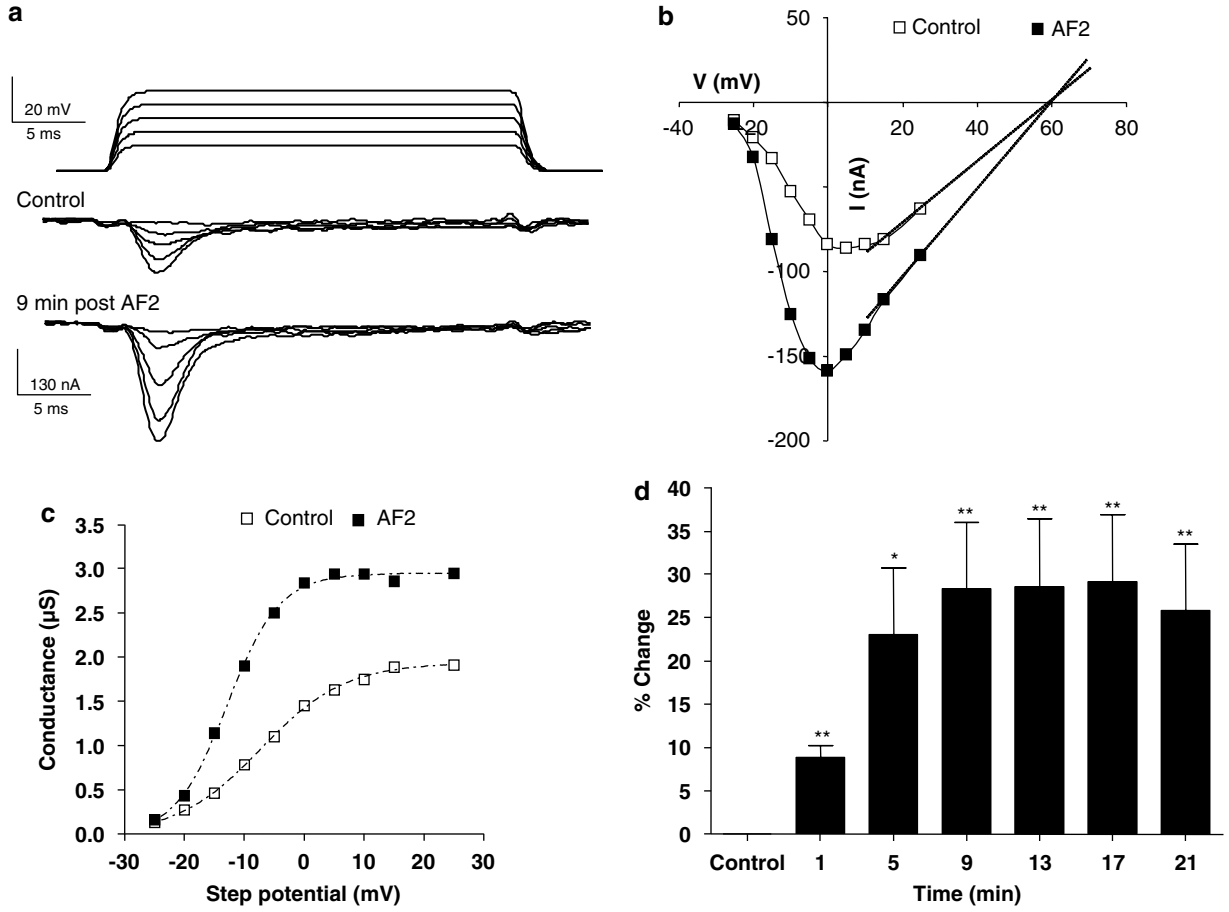

Figure 5 Transient inward currents show long-lasting potentiation after a 2-min application of 1 μM AF2. (**a**) Voltage-gated transient-inward currents recorded before and 9 min after AF2 application. Note the increase in the amplitude of the peak inward currents. (**b**) Peak-current step–voltage relationship for experiment shown in (**a**) control and 9 min after AF2 application. Last three current points of each plot were extrapolated to obtain the reversal potential, +59 mV. (**c**) Activation curve showing increase in G_{max}, a hyperpolarising shift in V_{50} and change in K_{slope} after AF2. (**d**) Long-lasting potentiation of the percentage change of the peak transient inward current after AF2 application (paired t-test, $n = 11$ preparations from separate worms, $^{**}P < 0.01$, $^{*}P < 0.05$).

lasted for more then 20 min after washing the AF2. We comment on the time-dependent nature of the increase in the discussion. Figure 5d shows the mean (±s.e.m.) percentage increases from 11 experiments. The mean potentiation for the 11 recordings after 17 min was 29±8%, with a wide variation of individual values ranging between 15–89%. In addition, we also examined the effect of the AF2 on the small-sustained inward current and found it to be without significant effect (nine preparations) illustrating the fact that AF2 had its major effect on the transient inward current.

AF2 did not affect inactivation of transient inward currents

The inactivation of the transient inward currents (Figure 6) was tested by using a pre-pulse protocol. The muscle cells were held at −35 mV, then taken to different pre-pulses for 130 ms to allow inactivation, and then finally stepped to a test-voltage of 0 mV. The pre-pulses were from −45 to 0 mV. The inactivation curves, produced by plotting the peak inward currents against the pre-pulse potentials, were fitted by the Boltzmann's equation; example pre-AF2 treatment and post-AF2 treatment inactivation curves are shown in Figure 6b. Overall, I_{max} had a value of −81.0±18.8 nA, before AF2 application and was −97.3±21.3 nA, after AF2 application (no significant change, $P>0.05$, $n=6$). V_{50} before AF2 application was −21.1±1.3 mV, and after AF2 application was −22.3±1.6 mV; no significant change, ($P>0.05$, $n=6$). In addition, the slope factor was not significantly different in the control, 6.4±0.7 mV, as compared to after AF2 application, 8.0±0.9 mV ($P>0.05$, $n=6$). These experiments showed that the exposure to AF2 did not affect the inactivation characteristics of the inward current.

The transient inward current is calcium dependent

We performed calcium substitution experiments to test effects on the transient inward current. Figure 7a shows representative recordings, where the amplitude of the transient inward current was reduced, reversibly, by removing calcium and bathing the preparation in a magnesium-Ringer solution for 10 min. The current returned towards normal on wash.

Figure 7b shows the current–voltage plots for this particular experiment. In six experiments, the peak current at 0 mV in the absence of calcium was significantly reduced from −123.3±11.7 to −21.7±13.7 nA, in the magnesium-Ringer solution. The inward current recovered to −80.8±13.4 nA, after perfusion with the control, calcium-Ringer solution for 10 min.

Figure 7c shows a bar chart of the peak currents at the step potential of 0 mV as a percentage of the control. These experiments showed that removal of the calcium reduced the inward current by 83% and suggested that most of the transient current is carried by calcium. In these experiments, we were not able to reversibly abolish all of the transient inward current despite bathing the preparations in calcium-free Ringer for more than 20 min. The remaining current suggests that a small proportion of the inward current is carried by other ions.

Effects of sodium and calcium substitution on the transient inward current

To examine the effect of sodium substitution on the transient inward current, we substituted both sodium and calcium with NMDG, as a nonpermeant cation. In the NMDG-Ringer (which contains no added calcium or sodium and would not support calcium or sodium currents), we found that there was only a small residual inward current and found that the addition of sodium could produce a modest increase in the amplitude of the inward current. However, only addition of calcium produced a large and significant increase in the transient inward current.

Figure 8a1 is a representative trace of the current in NMDG-Ringer, Figure 8a2 is a representative trace of the current trace following the addition of magnesium-Ringer (sodium present) and Figure 8a3 is the current trace following

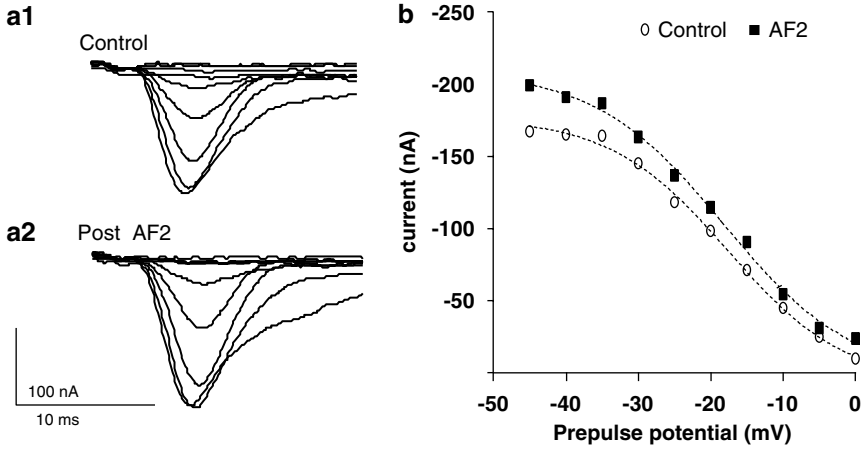

Figure 6 Effect of 1 μM AF2 on the inactivation of the transient inward current. The transient inward currents were activated by a test pulse of 0 mV following 130 ms pre-pulses of 45 mV, −40, −35, −30, −25, −20, −15, −10, −5 and 0 mV. (**a1**) A trace of control transient inward currents at 0 mV step potential after the pre-pulses. (**a2**) Transient inward currents at 0 mV step potential after the pre-pulses and following AF2 perfusion. (**b**) Shows the plot of peak current against the pre-pulse potential; the points were fitted to the inactivation curve as described by Boltzmann's equation.

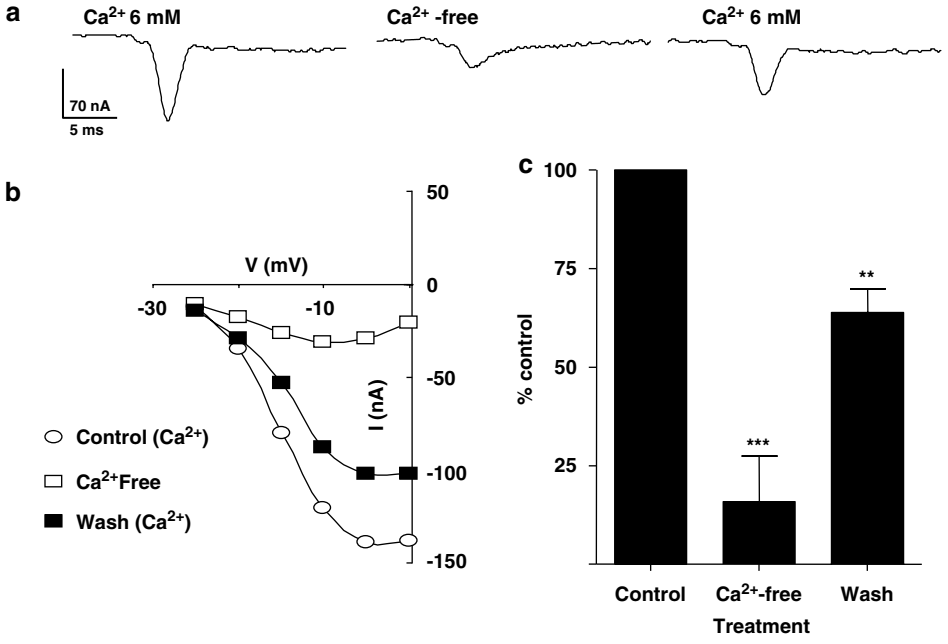

Figure 7 Calcium substitution decreases the amplitude of transient inward current. (**a**) Changes in voltage-gated transient inward currents before and after calcium substitution. (**b**) Current–voltage relationship (I–V) plot from the same experiment. (**c**) Calcium substitution significantly suppressed the inward current and the effect was reversible (paired *t*-test, $n=6$, $^{**}P<0.01$, $^{***}P<0.001$).

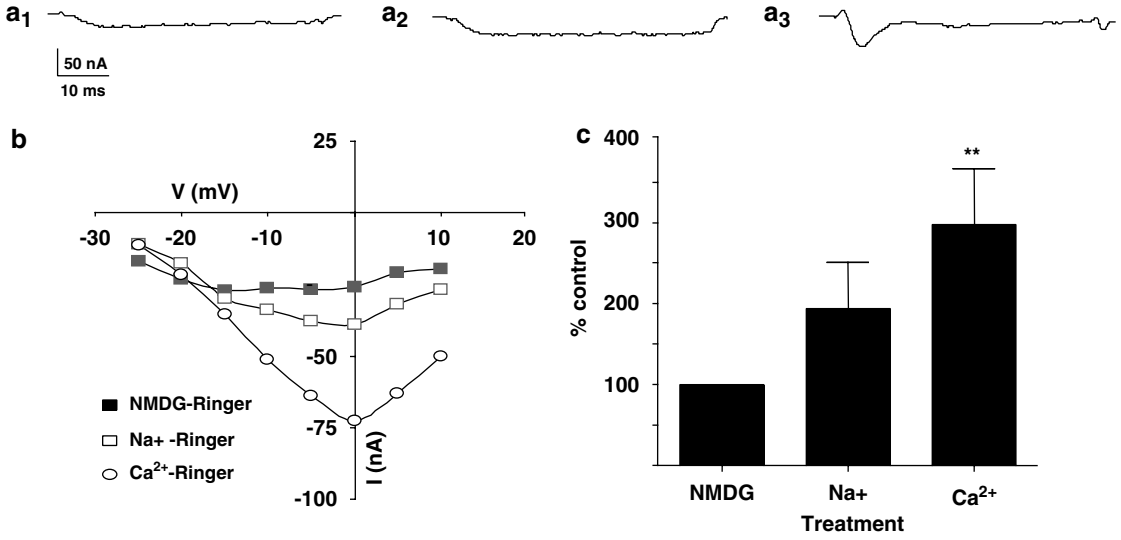

Figure 8 Effects of addition of sodium and calcium to NMDG-Ringer. (**a1**) A representative trace of inward currents in the absence of sodium and calcium (NMDG-Ringer). (**a2**) In the same preparation, a trace of inward currents in the presence of sodium (sodium-Ringer). (**a3**) In the same preparation, the transient inward current in the presence of sodium and calcium (calcium-Ringer). Note that only calcium produced a transient inward current. All currents are at −5 mV voltage step. (**b**) Current–voltage relationships for the inward currents—in the absence of both sodium and calcium, in the presence of sodium and when both sodium and calcium are present. (**c**) Mean percentage change in the peak transient inward current after addition of sodium and calcium. The inward currents for NMDG-Ringer were used for normalisation for each preparation. Only the addition of calcium produced a significant increase in normalised transient inward currents (paired *t*-test, $n=6$, $^{**}P<0.01$).

the addition of sodium and calcium when the muscle cell was in normal calcium-Ringer solution. The current-voltage relationship for this experiment is shown in Figure 8b. The peak inward current at 0 mV in NMDG-Ringer in this representative experiment was −26 nA; it increased to −39 nA following the addition of sodium; and increased to −73 nA when sodium and calcium were present (calcium-Ringer).

In six experiments, the peak transient inward current in NMDG-Ringer at 0 mV was -13.8 ± 5.3 nA. This current was -23.8 ± 3.1 nA in magnesium-Ringer (sodium present) and it increased to -37.2 ± 2.4 nA in calcium-Ringer. Figure 8c shows a bar chart of the currents expressed as a percentage of the control (NMDG-Ringer). The increase in the transient inward currents in calcium-Ringer was $260\pm69\%$ and was

significant ($P<0.01$, paired *t-test*, $n=6$). These experiments demonstrated that, in the absence of sodium and calcium, there was a small voltage-activated inward current. However, only the addition of calcium produced a large voltage-activated current. Sodium did not substitute for calcium. Subsequently, we will refer to this inward current as the voltage-activated calcium current.

Effect of calcium channel antagonists on transient voltage-activated calcium current

We have seen that most of the transient inward current is carried by calcium and that it is increased following AF2 treatment. We were interested to determine effects of some calcium channel antagonists, to see if the current had pharmacological properties that resembled mammalian calcium currents.

We tested effects of 10 mM cobalt on the voltage-activated calcium current (Figure 9). Figure 9a shows representative traces of the reversible inhibition of the calcium current. In this particular experiment, the current at 0 mV decreased from −78.3 (control) to – 6.2 nA in the presence of 10 mM cobalt; the current recovered to −78.0 nA after 25 min wash. Figure 9b shows the current–voltage plots from this experiment. Figure 9c shows a bar chart of normalised currents obtained from seven preparations before, during and at different times following wash. All of these experiments showed that 10 mM cobalt was effective at inhibiting the calcium current.

We also tested effects of 30 μM nickel, a T-type calcium channel antagonist and of 100 μM verapamil, a nonselective calcium channel antagonist (Figure 10). Both of these agents were without effect. These observations suggested that the pharmacology of the calcium current is different to that of vertebrates.

Effect of acetylcholine on the transient calcium current

There is evidence of muscarinic receptors present on *Ascaris* muscle (Colquhoun *et al*., 1991). We tested for the effects of

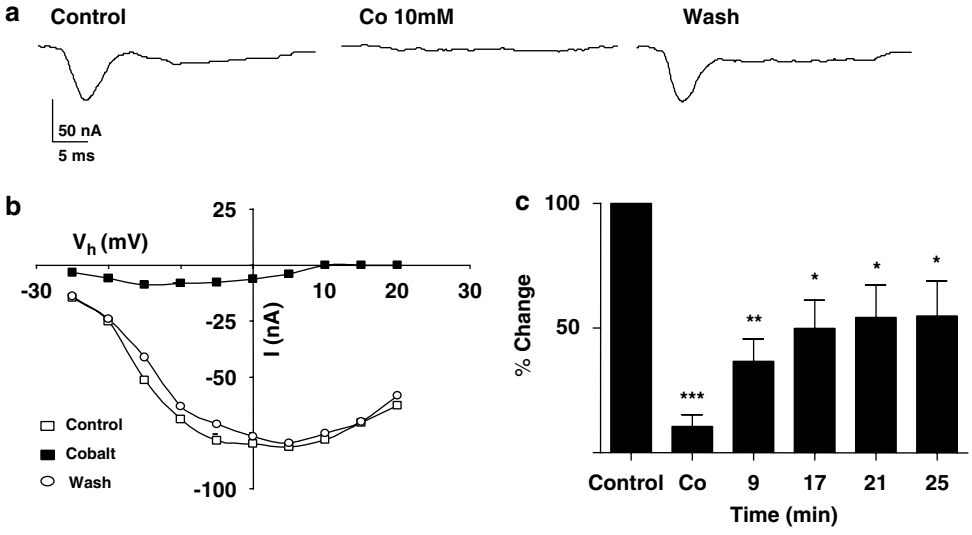

Figure 9 Cobalt blocked the transient inward currents. (**a**) An experiment representing effect of cobalt on transient inward current at 0 mV. (**b**) Current–voltage relationships for the inward currents before, after 10 mM cobalt application and after washing. (**c**) Cobalt application significantly suppressed the peak transient inward currents (paired *t*-test, $n=7$, $^{**}P<0.01$, $^{***}P<0.001$).

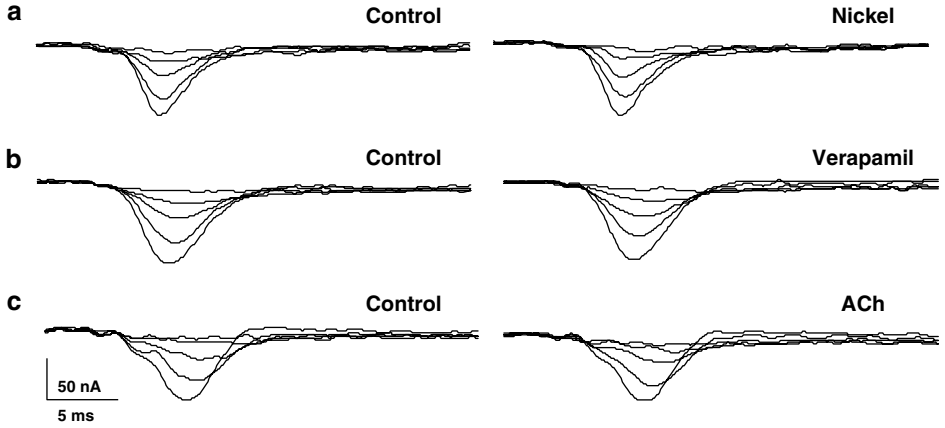

Figure 10 Lack of effect of nickel, verapamil and acetylcholine on transient inward current. Representative traces showing that application of (**a**) Nickel (30 μM). (**b**) Verapamil (100 μM) and (**c**) acetylcholine (ACh 1 μM) did not affect the transient inward current.

1 μM acetylcholine in six preparations and found no effects on the transient calcium current, suggesting that muscarinic receptors do not modulate calcium currents in *Ascaris* muscle.

Discussion

Spikes in Ascaris

Ascaris muscle is capable of producing full action potentials as well as partial spikes (DeBell *et al*., 1963). The spikes are suggested to start at the neuromuscular junction (syncytium) and then to travel to the bag region of the muscle via the arms of the muscle cell. Here, we can see that the bag region, from which we recorded, is capable of conducting voltage-activated currents to support spikes. The electrical activity and modulation of the spikes seen in *Ascaris* has been modelled by Turner (2001), who has shown that a combination of voltage-activated calcium currents, voltage-activated potassium currents (Martin *et al*., 1992) and calcium-activated chloride currents (Thorn and Martin, 1987) can produce repeating bursts of spikes in an oscillatory mode that is observed in fresh preparations (Weisblat *et al*., 1976). An increase in the calcium entry is predicted to change the pattern of this oscillation (Turner, 2001). In this manuscript, we have explored the effects of the neuropeptide, AF2, on the calcium currents.

AF2

Several groups have described how brief application of AF2 to *A. suum* muscle strips produces a long-lasting change in the contractility and electrical excitability and increases in muscle cyclic adenosine monophosphate (cAMP) (Cowden and Stretton, 1993; Pang *et al*., 1995; Reinitz *et al*., 2000; Maule *et al*., 2002; Trailovic *et al*., 2005). Trailovic *et al*. (2005) have also observed that brief (in contrast to maintained) application of AF2 results in long-lasting potentiation of depolarising responses to acetylcholine applied to *A. suum* muscle cells. This latter observation showed that AF2 has direct excitatory effects on *A. suum* muscle and appeared to contrast with earlier observations involving cut nerve cord experiments (Maule *et al*., 1995) that have suggested that AF2 has post-synaptic inhibitory effects on *Ascaris* muscle. However, these experiments involved removal of muscle synaptic receptors, so AF2 could interact with excitatory receptors on muscle that are removed with the nerve cords (Maule *et al*., 2002). We have described, here, how AF2 increases the amplitude and frequency of small spikes and large spikes. When we applied AF2 for a 2-min period to the muscle cells, we found that there was an increase in the transient inward current that lasted for more than 20 min after washout. AF2 produced an increase in the maximum and the threshold was shifted in the hyperpolarising direction. The increase in this inward current suggests it was responsible for the change in spontaneous depolarisations observed under current–clamp. The time-dependent and long-lasting effects of AF2 on acetylcholine responses and excitability has been discussed (Trailovic *et al*., 2005) and a putative mechanism involving activation of G-protein receptors and increases in calcium currents has been proposed. Here, we have been able to demonstrate the effect of AF2 on calcium currents. The small effect of AF2 on the total outward current (see Figure 3) suggests that the decreased outward current is not the primary cause of the increased excitability of the muscle cells.

The transient inward current is carried by calcium

We can say that the current producing the muscle spikes is mediated by voltage-activated calcium channels for the following reasons: the amplitude of *Ascaris* muscle spikes are reduced in low-Ca^{2+} Ringer solutions (Weisblat *et al*., 1976); the transient inward current is blocked by 1 mM lanthanum (Martin *et al*., 1992); removal of calcium reduces the amplitude of the transient inward current (see Figure 7); removal of sodium and calcium in the NMDG-Ringer abolishes the transient inward current; addition of calcium, but not sodium, allowed the transient current to reappear (see Figure 8); and addition of cobalt (Figure 9) abolished the transient current. All of these observations are consistent with calcium being the major, but not necessarily the exclusive charge carrier of the current. The reversal potential of the current in this series of experiment was estimated by extrapolation and was around $+45$ mV. The predicted Nernst calcium potential with 6 mM extracellular calcium and 1 μM intracellular calcium is $+110$ mV, some 65 mV more positive than we observed. Despite the prediction of a more positive reversal potential for calcium, others have made similar observations for the *C. elegans* L-type EGL-19, calcium channels (Jospin *et al*., 2002) and for the calcium channels in vertebrate preparations (Nowycky *et al*., 1985). Collectively, these observations suggest that the calcium channel in nematode and mammalian preparations is not exclusively permeable to calcium, but may also be permeable to other monovalent ions including sodium and potassium. Although we replaced all cations with NMDG, we found that a residual inward current remained in some preparations (Figure 8). This remaining inward current is not likely to be carried by cations (no permeable cations in NMDG-Ringer), so it may be produced by closing of outward calcium-dependent chloride channel current (Thorn and Martin, 1987), which is present in *Ascaris* bag cells. We did not investigate this current in NMDG further.

Comparison of voltage-activated calcium currents in mammals and Caenorhabditis elegans

Voltage-gated calcium channel currents in vertebrates can be divided into three major groups (Catterall, 2000).

(1) There is the T-type or transient calcium channel current that is activated at relatively negative potentials, $+70$ to -70 mV (V_{50} -51 mV, K 7.0 mV; Fox *et al*., 1987). It inactivates with a time constant in the 20–50 ms range at potentials more $+$ than -60 mV. The different types of calcium channels are built around a transmembrane ion-channel protein that is known as the α_1-subunit. Ca_V3 protein subunits are the α_1-subunit for the T-type channels (Perez-Reyes *et al*., 1998). A similar current has been described in the nematode *C. elegans* pharyngeal muscle, coded for by the gene *cca-1* that has around 70% similarity to mammalian Ca_V3 subunits (Mathews *et al*., 2003; Shtonda and Avery, 2005).

(2) There are the N-, P-, Q, and R-types of calcium currents that are activated at potentials +30 to −30 mV (N-type: V_{50} −6.5 mV, *K* 6.5 mV; Fox *et al*., 1987) and that inactivate in the 50–80 ms range. The N-type current is resistant to block by nickel and nifedipine. Cloned $Ca_V2.2$ subunits conduct N-type currents (Dubel *et al*., 1992); cloned $Ca_V2.1$ subunits (Mori *et al*., 1991) conduct P-/Q-type currents; cloned $Ca_V2.3$ subunits conduct R-type currents (Randall and Tsien, 1995). The *unc-2* gene of the nematode *C. elegans* has the greatest similarity to the $Ca_V2.3$ subunits (R-type current), but is also similar to $Ca_V2.1$ and $Ca_V2.2$ α_1-subunits (N- & Q/P-type currents).
(3) There is the L-type current that is activated by making bigger depolarising steps to potentials +10 to −10 mV (V_{50} +16.5 mV, *K* 5.5 mV; Fox *et al*., 1987). This current inactivates slowly with a time constant >500 ms. The L-type calcium current is mediated by the Ca_V1 family of α_1-subunits, inhibited by nifedipine, verapamil and potentiated by Bay K 8644. In *C. elegans*, body muscle and pharyngeal muscle, a current similar to the L-type current is conducted through a channel formed by an α_1-subunit coded for by the *egl-19* gene (Shtonda and Avery, 2005).

In the nematode, *C. elegans*, genes coding for α_1 calcium channel subunits are: *cca-1*, *unc-2* and *egl-19* (see above) and *nca1* and *nca2*. *nca1* and *nca2* are outliers, similar to one another, and to a channel in the yeast *Schiozosaccharomyces pombe* (Bargmann, 1998). They are found in the nervous system and ventral cord in *C. elegans*, but their electrophysiological properties have not yet been described.

Membrane potential, activation of Ascaris *and* C. elegans *calcium currents, and propagation distances*

The *C. elegans* body muscle has a resting membrane potential averaging −19.7 mV, so it is not surprising that there is only an L-type calcium (EGL-19) current present that requires potentials +20 to −20 mV to activate it (V_{50} +0.95, *K* 4.6 and E_{rev} +51 mV) (Jospin *et al*., 2002). The *C. elegans* L-type current is only partially blocked by a high (1 μm) concentration of nifedipine so it behaves differently to the mammalian L-type current. The *C. elegans* body wall muscle sometimes displays small spikes or overshooting action potentials (Jospin *et al*., 2002). In *C. elegans,* the pharyngeal muscle has a more negative equilibrium membrane potential of −53.6 mV (Shtonda and Avery, 2005) and it has both T-type (CCA-1) and L-type (EGL-19) currents. These currents support the large overshooting action potential of the pharynx. The more negative resting membrane potential allows activation of the T-type current.

The resting membrane potential of *Ascaris* muscle cells is around −35 mV, and displays both small spikes and overshooting action potentials along with slow waves. The voltage-activated current we observed has some but not all of the properties of the T- and L-type currents; it inactivated but required a relatively depolarised potential for activation and was not inactivated at a holding potential of −35 mV. The *Ascaris* calcium current was not inhibited by 30 μM nickel or 100 μM verapamil and was therefore pharmacologically different to T- and L-types of current (Fox *et al*., 1987; Jospin *et al*., 2002; Shtonda and Avery, 2005). The *Ascaris* calcium current has properties similar to the N-, P/Q- and R-types and was unlike currents carried by *C. elegans* EGL-19 and CCA-1. Sequence comparisons show that phenylalkylamine (verapamil) binding sites are present in *C. elegans,* in the EGL-19 L-type homologue (Snutch *et al*., 1991; Frøkjær-Jensen *et al*., 2006), but not in other *C. elegans* non-L-type calcium channel homologues. The *Ascaris* calcium current was most like the currents expected to be carried by UNC-2. The need for propagated spike activity in body muscle cells may be more important in a large nematode-like *A. suum*, where electrotonic conduction may not be sufficient to carry depolarisations over the larger distances, when compared to the much smaller *C. elegans*.

Significance of AF2 effects

A number of authors (Wolstenholme *et al*., 2004; Geary *et al*., 2004; Martin *et al*., 2005) have raised concerns about the development of resistance to existing anthelmintics. Our approach has been to investigate the actions of cholinergic anthelmintics (levamisole), to understand better the mode of action of these drugs and to develop a pharmacological strategy for countering resistance to these compounds. AF2 is found in different nematode species and its potency on the nematode neuromuscular system makes AF2 and its receptors attractive targets for the development of novel anthelmintic drugs. In muscle strips of *A. suum*, AF2 potentiates the contractile responses to acetylcholine and levamisole (Marks *et al*., 1999; Kubiak *et al*., 2003), increases spiking, post-synaptic neuromuscular potentials (Pang *et al*., 1995; Brownlee and Walker, 1999) and depolarising potentials in response to acetylcholine (Trailovic *et al*., 2005). These properties suggest that a synthetic AF2 ligand could be used to potentiate the effects of cholinergic anthelmintics like levamisole and so counter effects of resistance to these compounds. Lee *et al*. (1999) have synthesised a number of substituted 5-phenyl-1,3,4-thiadazoles, which bind to the *A. suum* AF2 receptor, some of which show activity in a *C. elegans* motility assay; potentiation of cholinergic anthelmintics with these compounds has not yet been studied. From our results, it is clear that AF2 could potentiate contractions induced by cholinergic anthelmintics, at least in part, by increasing the entry of calcium through voltage-activated channels. We have not studied the mechanism of the coupling to the calcium channels, but it is possible that cAMP and protein kinase A are involved (Catterall, 2000), as AF2 is known to significantly elevate cAMP in *A. suum* muscle (Reinitz *et al*., 2000; Thompson *et al*., 2003). Other mechanisms by which AF2 may potentiate muscle contraction remained to be investigated.

Acknowledgements

We acknowledge the support of the NIH to RJM: RO1 A1047194

Conflict of interest

The authors state no conflict of interest.

References

Bargmann CI (1998). Neurobiology of the *Caenorhabditis elegans* genome. *Science* **282**: 2028–2033.

Brownlee DJ, Walker RJ. (1999). Actions of nematode FMRFamide-related peptides on the pharyngeal muscle of the parasitic nematode, *Ascaris suum*. *Ann NY Acad SCI* **897**: 228–238.

Catterall WA (2000). Structure and regulation of voltage-gated Ca^{2+} channels. *Annu Rev Cell Dev Biol* **16**: 521–555.

Colquhoun L, Holden-Dye L, Walker RJ (1991). The pharmacology of cholinoceptors on the somatic muscle cells of the parasitic nematode *Ascaris suum*. *J Exp Biol* **158**: 509–530.

Cowden C, Stretton AO (1993). AF2, an *Ascaris* neuropeptide: isolation, sequence, and bioactivity. *Peptides* **14**: 423–430.

DeBell JT, Del Castillo J, Sanchez V (1963). Electrophysiology of the somatic muscle cells of *Ascaris lumbricoides*. *J Cell Physiol* **62**: 159–177.

Dent JA, Smith MM, Vassilatis DK, Avery L (2000). The genetics of ivermectin resistance in *Caenorhabditis elegans*. *Proc Natl Acad Sci USA* **97**: 2674–2679.

Dockray GJ (2004). The expanding family of -RFamide peptides and their effects on feeding behaviour. *Exp Physiol* **89**: 229–235.

Dubel SJ, Starr TV, Hell J, Ahlijanian MK, Enyeart JJ, Catterall WA *et al*. (1992). Molecular cloning of the alpha-1 subunit of an omega-conotoxin-sensitive calcium channel. *Proc Natl Acad Sci USA* **89**: 5058–5062.

Fox AP, Nowycky MC, Tsien RW (1987). Single-channel recordings of three types of calcium channels in chick sensory neurones. *J Physiol* **394**: 173–200.

Frøkjær-Jensen C, Kindt KS, Kerr RA, Suzuki H, Melnik-Martinez K, Gerstbreih B *et al*. (2006). Effects of voltage-gated calcium channel subunit genes on calcium influx in cultured *C. elegans* mechanosensory neurons. *J Neurobiol* **66**: 1125–1139.

Geary TG, Conder GA, Bishop B (2004). The changing landscape of antiparasitic drug discovery for veterinary medicine. *Trends Parasitol* **20**: 449–455.

Geary TG, Marks NJ, Maule AG, Bowman JW, Alexander-Bowman SJ, Day TA *et al*. (1999). Pharmacology of FMRFamide-related peptides in helminths. *Ann NY Acad Sci* **897**: 212–227.

Geerts S, Gryseels B (2001). Anthelmintic resistance in human helminths: a review. *Trop Med Int Health* **6**: 915–921.

Greenwood K, Williams T, Geary T (2005). Nematode neuropeptide receptors and their development as anthelmintic screens. *Parasitology* **131** (Suppl): S169–S177.

Jospin M, Jacquemond V, Mariol MC, Segalat L, Allard B (2002). The L-type voltage-dependent Ca^{2+} channel EGL-19 controls body wall muscle function in *Caenorhabditis elegans*. *J Cell Biol* **159**: 337–348.

Kubiak TM, Larsen MJ, Davis JP, Zantello MR, Bowman JW (2003). AF2 interaction with *Ascaris suum* body wall muscle membranes involves G-protein activation. *Biochem Biophys Res Commun* **301**: 456–459.

Lee BH, Dutton FE, Clothier MF, Bowman JW, Davis JPJohnson SS, Thomas EM *et al*. (1999). Synthesis and biological activity of anthelmintic thiadiazoles using an AF2 receptor binding assay. *Bioorg Med Chem Lett* **21**: 1727–1732.

Marks NJ, Shaw C, Maule AG, Davis JP, Halton DW *et al*. (1995). *Isolation of AF2 (KHEYLRFamide) from Caenorhabditis elegans*: evidence for the presence of more than one FMRFamide related peptide-encoding gene. *Biochem Biophys Res Commun*. **217**: 845–851.

Marks NJ, Sangster NC, Maule AG, Halton DW, Thompson DP, Geary TG *et al*. (1999). Structural characterisation and pharmacology of KHEYLRFamide (AF2) and KSAYMRFamide (PF3/AF8) from *Haemonchus contortus*. *Mol Biochem Parasitol* **100**: 185–194.

Martin RJ, Thorn P, Gration KA, Harrow ID (1992). Voltage-activated currents in somatic muscle of the nematode parasite *Ascaris suum*. *J Exp Biol* **173**: 75–90.

Martin RJ, Verma S, Levandoski M, Clark CL, Qian H, Stewart M *et al*. (2005). Drug resistance and neurotransmitter receptors of nematodes: recent studies on the mode of action of levamisole. *Parasitology* **131** (Suppl): S71–S84.

Mathews EA, Garcia E, Santi CM, Mullen GP, Thacker C, Moerman DG *et al*. (2003). Critical residues of the *Caenorhabditis elegans* *unc-2* voltage-gated calcium channel that affect behavioral and physiological properties. *J Neurosci* **23**: 6537–6545.

Maule AG, Geary TG, Bowman JW, Marks NJ, Blair KL, Halton DW *et al*. (1995). Inhibitory effects of nematode FMRFamide-related peptides (FaRPs) on muscle strips from *Ascaris suum*. *Invert Neurosci* **1**: 255–265.

Maule AG, Mousley A, Marks NJ, Day TA, Thompson DP, Geary TG *et al*. (2002). Neuropeptide signaling systems - potential drug targets for parasite and pest control. *Curr Top Med Chem* **2**: 733–758.

Maule AG, Shaw C, Bowman JW, Halton DW, Thompson DP, Geary TG *et al*. (1994). The FMRFamide-like neuropeptide AF2 (*Ascaris suum*) is present in the free-living nematode, *Panagrellus redivivus* (Nematoda, Rhabditida). *Parasitology* **109** (Part 3): 351–356.

Mori Y, Friedrich T, Kim M-S, Mikami A, Nakai J, Ruth P *et al*. (1991). Primary structure and functional expression from complementary DNA of a brain calcium channel. *Nature* **350**: 398–402.

Mousley A, Maule AG, Halton DW, Marks NJ (2005). Inter-phyla studies on neuropeptides: the potential for broad-spectrum anthelmintic and/or endectocide discovery. *Parasitology* **131** (Suppl): S143–S167.

Nowycky MC, Fox AP, Tsien RW (1985). Three types of neuronal calcium channel with different calcium agonist sensitivity *Nature*. **316**: 440–443.

Pang FY, Mason J, Holden-Dye L, Franks CJ, Williams RG, Walker RJ (1995). The effects of the nematode peptide, KHEYLRFamide (AF2), on the somatic musculature of the parasitic nematode *Ascaris suum*. *Parasitology* **110** (Part 3): 353–362.

Perez-Reyes E, Cribbs LL, Daud A, Lacerda AE, Barclay J, Williamson MP *et al*. (1998). Molecular characterization of a neuronal low-voltage-activated T-type calcium channel. *Nature* **391**: 896–900.

Pittaway KM, Rodriguez RE, Hughes J, Hill RG (1987). CCK 8 analgesia and hyperalgesia after intrathecal administration in the rat: comparison with CCK-related peptides. *Neuropeptides* **10**: 87–108.

Randall A, Tsien RW (1995). Pharmacological dissection of multiple types of Ca2 + channel currents in rat cerebellar granule neurons. *J Neurosci* **15**: 2995–3012.

Reinitz CA, Herfel HG, Messinger LA, Stretton AO (2000). Changes in locomotory behavior and cAMP produced in *Ascaris suum* by neuropeptides from *Ascaris suum* or *Caenorhabditis elegans*. *Mol Biochem Parasitol* **111**: 185–197.

Shtonda B, Avery L (2005). CCA-1, EGL-19 and EXP-2 currents shape action potentials in the *Caenorhabditis elegans* pharynx. *J Exp Biol* **208**: 2177–2190.

Snutch TP, Tomlinson WJ, Leonard JP, Gilbert MM (1991). Distinct calcium channels are generated by alternative splicing and are differentially expressed in the mammalian CNS. *Neuron* **7**: 45–57.

Stretton AOW, Cowden C, Sithigorngul P, Davis RE (1991). Neuropeptides in the nematode *Ascaris suum*. *Parasitology* **102** (Suppl): S107–S116.

Thiemermann C, al-Damluji S, Hecker M, Vane JR (1991). FMRF-amide and L-Arg-L-Phe increase blood pressure and heart rate in the anaesthetised rat by central stimulation of the sympathetic nervous system. *Biochem Biophys Res Commun* **175**: 318–324.

Thompson DP, Davis JP, Larsen MJ, Coscarelli EM, Zinser EW, Bowman JW *et al*. (2003). Effects of KHEYLRFamide and KNEFIR-Famide on cyclic adenosine monophosphate levels in *Ascaris suum* somatic muscle. *Int J Parasitol* **33**: 199–208.

Thorn P, Martin RJ (1987). A high-conductance calcium-dependent chloride channel in *Ascaris suum* muscle. *Q J Exp Physiol* **72**: 31–49.

Trailovic SM, Clark CL, Robertson AP, Martin RJ (2005). Brief application of AF2 produces long lasting potentiation of nAChR responses in *Ascaris suum*. *Mol Biochem Parasitol* **139**: 51–64.

Turner RE (2001). A model for an *Ascaris* muscle cell. *Exp Physiol* **86**: 551–559.

Weisblat DA, Byerly L, Russell RL (1976). Ionic mechanisms of electrical activity in somatic muscle of the nematode *Ascaris lumbricoides*. *J Comp Physiol* **111**: 93–113.

Wolstenholme AJ, Fairweather I, Prichard R, von Samson-Himmelstjerna G, Sangster NC (2004). Drug resistance in veterinary helminths. *Trends Parasitol* **20**: 469–476.